An acoustic technique for Lagrangian velocity measurements

Nicolas Mordant, Pascal Metz, Jean-François Pinton, Olivier Michel

Acoustical technique for Lagrangian velocity measurement

Nicolas Mordant
Laboratoire de Physique Statistique, Ecole Normale Supérieure, CNRS-UMR 8550, 24 Rue Lhomond, 75231 Paris Cedex 05, France

Pascal Metz and Jean-François Pinton
Laboratoire de Physique, Ecole Normale Supérieure de Lyon, CNRS-UMR 5672, 46 Allée d'Italie, F-69364 Lyon Cedex 07, France

Olivier Michel
Laboratoire d'Astrophysique, CNRS-UMR 6525, Université de Nice, Parc Valrose, F-06108 Nice, France

(Received 13 May 2004; accepted 5 November 2004; published online 10 January 2005)

Ultrasonic transducers array can be used to track solid particles advected by a turbulent flow. The simultaneous use of four linear antennas of transducers gives the 3D position of the particles. The extraction of the Doppler frequency shift gives a precise estimation of velocity components. We describe the principle of the technique, the signal conditioning and the acquisition schemes. We show briefly the performances of the technique applied to a turbulent flow at high Reynolds number. The dynamical range of the measurement is over 55 dB and the frequency response spans over 2 decades. These performances allow us to investigate the inertial time scales of Lagrangian turbulence. © *2005 American Institute of Physics.* [DOI: 10.1063/1.1844452]

I. INTRODUCTION

In fluid mechanics research, one traditionally measures flow characteristics in Eulerian variables. This is the case for example of the velocity field for which one seeks instantaneous or time averages of spatial profile $u(x,t)$. Besides traditional techniques such as hot-wire anemometry and laser-Doppler velocimetry that yield single point Eulerian measurements,[1] spatially extended techniques are now widely used. High performance Particle Image Velocimetry (PIV) (Ref. 2) and holographic PIV (Ref. 3) now give two- and three-dimensional pictures of the flow field that are currently used in aerodynamics, and have contributed to the development of sub-grid-scale modeling used in numerical simulations. On the other hand, various aspects of fundamental and applied fluid mechanics research have shown the need to develop measurement of Lagrangian properties of the flow. In this case, one seeks to measure the flow variables following the motion of individual fluid particles. This is important to understand the physics of mixing where particle dispersion, and thus efficiency, stems from the complexity of the particle motion. It appears to be essential in problems where Lagrangian characteristics controls the dynamics, such as rain formation in clouds[4] or combustion.[5] From a fundamental point of view, recent theoretical developments have shown that the intermittency property of turbulent flows could be better understood from the Lagrangian point of view.[6] Thus there has been a strong motivation to develop experimental measurement of the Lagrangian motion of fluid particles.

In the case of two-dimensional turbulence, measurements have been obtained[7] using Particle Tracking Velocimetry techniques, in which small tracer particles are filmed in their planar motion using fast video cameras. For 3D measurements, optical methods are limited due to the formidable amount of data that must be generated: in a turbulent flow, the scales of motion cover a range that grows as $\mathrm{Re}^{3/4}$, if Re is the Reynolds number of the flow. Thus, if one wants to resolve all the scales of three-dimensional motion, one needs over $\mathrm{Re}^{9/4}$ pixels that must be refreshed and recorded on the smallest time scale of motion. For example, at a Reynolds number of 10^4, common in engineering applications, this approach would generate over one terabyte of data per second. It is currently out of reach with the existing technology of digital cameras and acquisition devices. As a result, optical detection of a Lagrangian motion, usually referred to as "Particle Tracking Velocimetry" has been limited to moderately turbulent flows[8,9] or to restricted descriptions of highly turbulent flows, such as the determination of the acceleration of tracer particles.[10]

It is therefore desirable to develop a device to perform high-resolution tracking of Lagrangian motion covering the entire range of scales. We present here a new technique, based on acoustics, which independently measures the position and velocity of single tracer particles. Compared to optical techniques, the limitation is that only one (or a few) particles are tracked. The advantage is that their motion is completely resolved: as detailed below, this technique can follow particles of a 250 μm at a time resolution of 0.5 ms, for times up to several seconds. Its acoustic nature allows for application in flows using nontransparent fluids. In Sec. II, we describe the fundamentals of our technique and experimental constraints together with the acoustic and electronics parts, the data acquisition and data processing schemes. Section III is devoted to a brief analysis of the performances of our technique—a complete report of our findings in the context of turbulence studies and comparison with Direct Numerical Simulations is given elsewhere.[11]

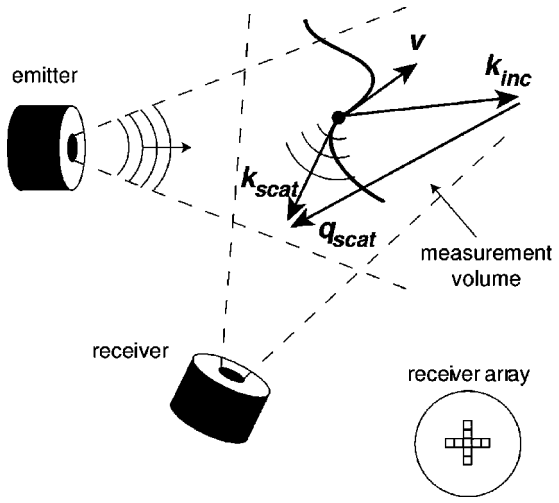

FIG. 1. Principle of the measurement: a monochromatic wave is emitted in the flow. A solid particle advected by the flow scatters the incoming wave. The scattered sound is continuously recorded by an array of receivers constituted in 9 transducers disposed on a cross.

II. MEASUREMENT TECHNIQUE

A. Principle

The principle of the measurement is sketched in Fig. 1. When a particle is continuously insonified with a monochromatic acoustic wave, the scattered sound is Doppler shifted by an amount proportional to the velocity of the particle. If this scattering signal is recorded by an array of transducers, the detection of the phase shift between array elements gives the position of the particle while the detection of the Doppler shift yields the velocity of the particle. One has thus access to an independent and direct measurement of both the position and the velocity of the tracer particle. The detection of the direction of scattering (i.e., of the particle position) using arrays of transducers follows a standard procedure in Radar-type array detection. In contrast, the tracking of the instantaneous Doppler shift requires the implementation of a complex signal processing scheme. This is because in order to obtain the velocity information, one needs to track the evolution of a frequency (the Doppler shift) as a function of time. Appropriate time-frequency numerical schemes have to be implemented. In this section we define the expected performance of the measurement and we discuss the implementation of the tracking technique: amplitude of acoustic scattering, data acquisition and processing. Its application to the detection of the motion of a Lagrangian tracer particle in a turbulent flow will be discussed in the next section. Note that for low Reynolds number flows, where relative Doppler shifts are small, one could use standard ultrasonic Doppler measurements which analyze the echoes from pulse wavetrains,[12] as in now commercially available anemometers. However, the pulse repetition-rate of these devices is too low for the rapidly varying flow we wish to consider and we choose to operate with a continuous insonification.

B. Measurements requirements

In the actual experimental implementation, parameters such as transducer size, emission frequency, precision of data acquisition and signal processing scheme are chosen according to the expected performance of the instrument. Our primary goal was to be able to study turbulent flows and we thus discuss the requirements in this context; however our discussion is quite general and can easily be extended to other flows.[13]

Let us consider a typical turbulent flow generated in laboratory conditions. For example, a water flow with a Reynolds number of $\mathrm{Re}=10^5$ and an integral length scale $L=5$ cm (characteristic scale of the energy injection, the actual size of the flow can be larger), the characteristics are:[14]

(1) The scales of motions in space range from L to the dissipative length $\eta=L/\mathrm{Re}^{3/4}\sim 10$ μm, with the velocity gradients peaking at about the Taylor microscale $\lambda=\sqrt{15}L/\mathrm{Re}^{1/2}\sim 0.6$ mm;
(2) The velocities in the flow vary in a continuous range from the large scale $U=\nu\,\mathrm{Re}/L\sim 1$ m/s ($\nu=10^{-6}$ m^2/s is the kinematic viscosity of the water) to the value at small scale $u_\eta=U/\mathrm{Re}^{1/4}\sim 5$ cm/s;
(3) The time scales of motion range from the integral scale at which the flow is set into motion, $T=L/U\sim 0.05$ s, to the fast turnover time of the smallest eddies, $\tau_\eta\sim T/\mathrm{Re}^{1/2}\sim 0.2$ ms.

We wish to track the motion of a tracer particle for time and space scales ranging from the large (slow) scales of motion down to the smallest (and fastest) scales that can possibly be resolved by our instrument. It is implicit that the particle's density should match that of the fluid, and that its acoustic impedance should be quite different so as to maximize the scattering effect. Ideally, one would like to track particles with a size equal to the dissipative length, 10 microns, at a time resolution equal to 0.1 ms for a duration of over 1 s. Due to the weakness of the acoustic scattering, this is not possible and we shall restrict ourselves to the tracking of particle that have a size larger than the Kolmogorov dissipation length ($\eta\sim 10$ μm) but smaller than the Taylor microscale of the flow ($\lambda\sim 600$ μm). The corresponding time scale of motion lies between the integral time ($T\sim 0.05$ s) and the eddy turnover time at the Taylor scale, $\tau_\lambda=3$ ms. In this way, the inertial range of the turbulent motion is nearly fully resolved.[14] In practice, we require that the measurement technique be able to follow a 250 μm particle with a time resolution of 1 ms, during a motion that spans a volume larger than $L^3\sim(5\ \mathrm{cm})^3$, with a duration up to 1 s.

Note again at this point that trying to meet these requirements using optical techniques would require digital cameras with a pixel array larger than 1000^2 pixels ($\equiv 10$ cm/100 μm), an acquisition rate of the order of 10 kHz (the particle velocity is obtained as the derivative of the position so oversampling is necessary), and the ability to record sequences of up to 10 000 such images. While this will be in principle within reach of technology in the near future, our acoustic technique provides a lower cost alternative.

C. Acoustic scattering

Let us first analyze the velocity detection scheme, i.e., the detection of the Doppler shift in the sound scattered by a

moving particle. The incident wave is emitted with pulsation ω_0 by a small transducer at the flow wall. The Doppler shift measured by the transducer is thus:

$$2\pi f = \Delta\omega(t) = \mathbf{q} \cdot \mathbf{v}_p(t), \tag{1}$$

where $\mathbf{v}_p$ and $\mathbf{q}$ are the velocity and scattering wave vector $\mathbf{q}=\mathbf{k}_{\text{scat}}-\mathbf{k}_{\text{inc}}$. The acoustic wavelength is $\lambda_w = 2\pi/k_{\text{inc}}$.

Once the frequency of the incident sound is chosen, the size of the transducers result from the following compromise: (i) small transducers insonify or detect sound from a large portion of the flow volume, where the particle motion can be tracked; (ii) the amplitude of the emission and the sensitivity of the detection decrease with the area of the transducer. There are also limitations in the achievable size of the piezoelectric transducers and their central resonant frequency. We use square transducers with a $\Lambda = 2$ mm side length, with a resonance frequency centered at either 2.5 MHz or 2.8 MHz. The receiver array has the geometry of a cross, as shown in Fig. 1. The detection of the phase shift between each element of one line of the array gives one angle of scattering. With the two cross lines, the direction a line of emission (Tracer-Receiver) is reconstructed. The position of the particle is obtained using two such arrays probing perpendicular directions. In order to avoid too large amplitude oscillations, the scattering volume should be in the far field region of the emitting and receiving transducers, that is at distances larger than $\Lambda^2/\lambda_w \sim 10$ mm.

D. Signal conditioning and acquisition

A relatively small transducer probes a large region of space (the main diffraction lobe of a 2 mm transducer spans 35°), and also generates echoes from the boundaries of the flow. Even if the flow walls are covered with sound absorbing material (see the experimental setup section) one expects the echoes to have a larger amplitude than the sound scattered by the moving tracer particle. Indeed we observe that the echoes are 60 dB larger than the scattered sound. If one requires a 60 dB resolution on the scattered amplitude (as an instrument standard) the signal from the piezoelectric transducers must be conditioned and sampled with devices that preserve a 120 dB dynamical range. With frequencies of sound of about 2.5 MHz, one should use digitizers with at least 20 bits of resolution at a sampling frequency of 10 MHz. Such devices exist (HPE1430 by Agilent Technologies) but their cost prevents using one unit per acquisition channel (recall that in this experiment, 2 arrays of 9 transducers are used).

However, it can be taken advantage of the fact that, for each transducer, the signal has a narrow frequency support Δf so that the effective Nyquist sampling rate is $2\Delta f$ only, leading to an overall minimal sampling frequency equal to $2K\Delta f$ in the case of K channels to be sampled. We thus propose, as an alternative strategy, to perform an heterodyne detection of the channels together with frequency multiplexing. Each channel is frequency shifted into an individual frequency band with a lock-in amplifier and then all channels are summed, cf. Fig. 2. In this process, it is essential to preserve the synchronicity of the signals. The signal conditioning for a single channel is sketched in Fig. 2(b). The

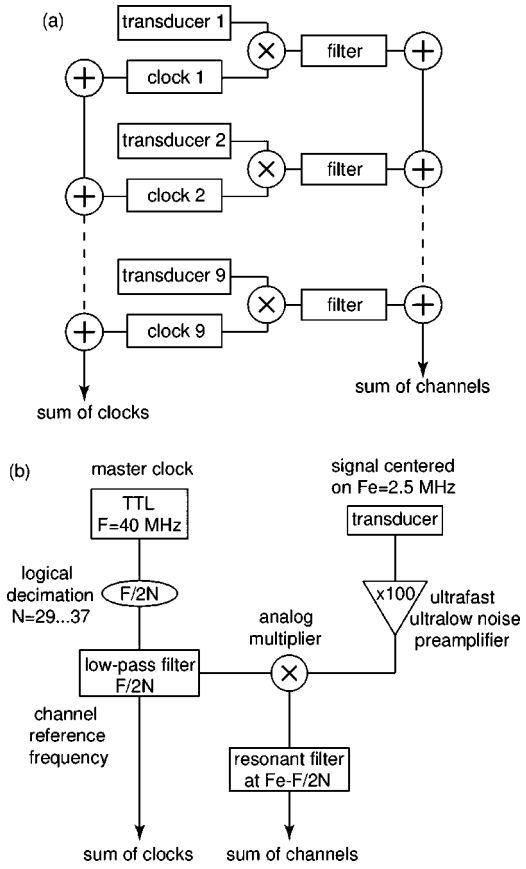

FIG. 2. Signal conditioning. (a) Principle: the signals from the 9 transducers in each transducer array are multiplied by 9 clocks at different frequencies, and summed into a single channel. The same is done for the 9 reference clocks which have to be recorded for data postprocessing; (b) detail of the analog processing in each channel: the reference clock is generated by decimation of a master TTL clock and then low-pass filtered to suppress the harmonics. The preamplified signal coming from the transducer is then analogically multiplied by the reference clock signal in order to shift the measurement to a lower preset frequency band. The result is then sent to a resonant filter that amplifies the target preset frequency band.

signal from the transducer is preamplified before heterodyning. The latter part is achieved using a four quadrant analog multiplier. The heterodyning frequency is built from a master clock (which also drives the emitter) using a logical decimator. After multiplication, the signal is bandpass filtered; a resonant circuit with a bandwidth of 20 kHz is used. The purpose of the resonant circuit is to amplify the heterodyned signal so that its amplitude becomes larger than the sum of the noise of the 8 other channels.

The performance of the preamplifier, heterodyning channels and summation are shown in Fig. 3. First, Fig. 3(a) gives the spectra of the signals from each of the nine transducer channels; in this case the conditioning unit is not connected to the transducers but to an equivalent 50 Ω impedance: the noise base level of each channel is at −160 dB and the resonant circuit has an effective amplification of 20 dB. When the transducers are now connected to the conditioning unit in a flow at rest, with an incident sound at 2.8 MHz, the power spectrum of the summed output signal has the form shown in Fig. 3(b): the center frequency of each channel is marked with a cross and the base level is at −155 dB. When the flow is set into motion the power spectrum of the signal after

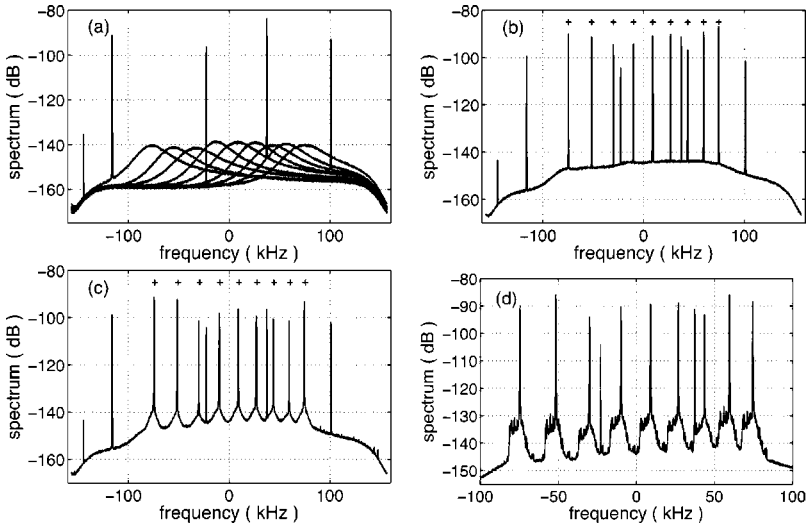

FIG. 3. Power spectra (in dB) of the signals in the analog processing; *x*-axis are in units of kiloHertz, with zero the center of the frequency band to be digitized. (a) Superimposed spectra from of each conditioning channel with the input connected to a 50 Ohm reference impedance. The sharp peaks are spurious harmonics of the master clock that are easily filtered out at the digital signal processing stage. (b) Power spectrum of the output of the conditioning unit when the transducers are connected, the incident sound turned on, while the flow is at rest; the crosses mark each of the 9 transducers; the signal is made of the peaks at the emission frequency due to the reflections and the noise of the electronics. (c) Same when the flow is established; the slight broadening of the bottom of the peaks is induced by the velocity gradients in the flow (Ref. 16). (d) Same with tracer particles introduced into the flow; note that the signal due to the motion of the tracer particles is some 60 dB below the echos detected in the absence of fluid motion.

summation becomes that of Fig. 3(c); when comparing to Fig. 3(b), two features are clearly visible: each central line is slightly broadened from the Doppler shift induced by the velocity gradients on the echoes of the incident sound, and the noise base level is augmented, presumably due to the scattering of sound from the velocity gradients. Finally, when tracer particles are introduced into the flow, the spectrum takes the form of Fig. 3(d). The sharp Doppler broadening comes from the scattering from the beads, in this case the maximum shift is of about 5 kHz, which corresponds to a particle velocity of about 2 m/s. Note that all transducers record the same spectrum, and that the level of the signal is a mere 10–20 dB above the level it has in the absence of tracer particles. This poor signal-to-noise ratio must be taken into account in the signal processing algorithm which extracts the instantaneous Doppler shift of the sound scattered by the particles. It is described in the next section.

E. Signal processing: Velocity tracking

For velocities of order 1 m s^{-1}, the Doppler shift Δf is of the order of 2.5 kHz in the geometry chosen for our experiment. We also require a time resolution Δt of the order of 1 ms. These requirements imply that Fourier-based methods cannot be used because the Shannon constraint $\Delta t \cdot \Delta f > 1$ imposes a frequency resolution of order 1 kHz which is not good enough for a measurement. To overcome this intrinsic limitation of the Fourier transform, one has to add *a priori* information on the structure of the signal. As a matter of fact, we know its structure: the sound received from each particle is a complex exponential whose amplitude is slowly varying as a function of the particle position in the beam and whose frequency is more rapidly varying (the velocity and thus the Doppler shift has a faster dynamics than the position). Thus the sound recorded by each transducer may be expressed in the following way:

$$x(t) = \sum_m a_m(t) \exp\left(j2\pi \int_0^t f_m(s)\mathrm{d}s + j\phi_m \right) + n(t), \qquad (2)$$

where a_m is the amplitude of the sound scattered on the detector by the particle m, f_m is the instantaneous Doppler frequency. The signal also contains some noise $n(t)$ that is supposed to be Gaussian white noise, in a first order approximation. The signal processing task is thus turned into a parametric estimation problem, which we solve using an approximated maximum likelihood (AML) approach. The algorithm and its performances are described in detail in a previous paper.[15] The algorithm is coupled to a prediction/correction algorithm to enhance the tracking performance. It can be seen as a generalized Kalman filter. An example of a single channel raw time series and corresponding frequency modulation after AML processing is displayed in Fig. 4. The measurement is made in the setup and with flow conditions as described in Sec. III.

F. Signal processing: Position tracking

The design of a transducer array is such that it forms two orthogonal linear antennas (Fig. 1). Consider the case of a distant source in a direction forming an angle θ relative to the axis of one antenna. The sound recorded by two consecutive array elements has the relative phase shift

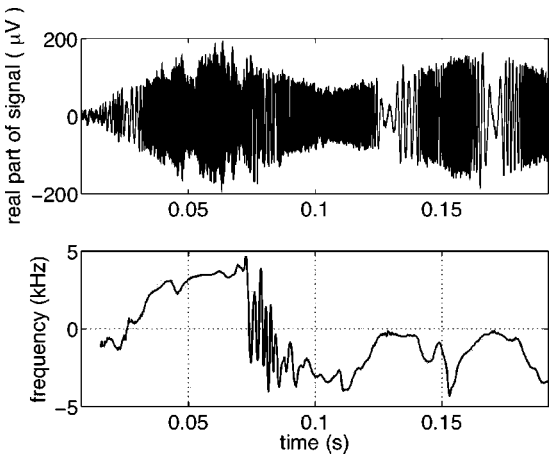

FIG. 4. Example of experimental time series. The signal is scattered by a 250 μm particle advected in a turbulent flow. (Top) Real part of the heterodyned acoustic signal, from one transducer. Fast oscillations correspond to large Doppler shifts and hence large particle velocities. (Bottom) Corresponding frequency modulation extracted by the AML processing algorithm (in this case signals from the nine transducers have been used).

$$\phi = \frac{\omega d \cos\theta}{c}, \tag{3}$$

where ω is the pulsation of the source, d is the distance between transducers, and c is the celerity of the sound. Thus the problem of estimation of the angle θ is equivalent to the estimation of a spatial frequency equal to

$$f_s = \frac{\omega \cos\theta}{c}, \tag{4}$$

so that the AML algorithm can again be applied to extract the direction of arrival of the sound. Each linear antenna in a transducer array thus yields a direction of sound scattering so that with two linear antennas one obtains a line of sound emission. In our setup where two such arrays are used, we obtain two lines that intersect in space at the position of the particle. Note that because this position reconstruction is based on the relative phase between transducers, it requires the accurate knowledge of the relative phase of the different clocks used in the analog multiplexing stage.

G. Precision of the measurement

We now analyze in some detail the precision of the measurement of the particle velocity and position. We begin with the velocity, related to a sound frequency Doppler shift by the relationship $2\pi f = \mathbf{q}\cdot\mathbf{v}_p$, cf. Eq. (1). The scattering wave vector $\mathbf{q}$ is computed as the difference between the incoming wave vector $\mathbf{k}_{\text{scat}} - \mathbf{k}_{\text{inc}}$. It is uniquely defined only when the incident and scattered waves have plane wave fronts. This is not the case in the experiment because the acoustic transducers have a finite aperture Λ (Sec. II C and Fig. 1 and 5). The scattering wave vector $\mathbf{q}$ thus varies within $\mathbf{q} \pm \delta\mathbf{q}$, and this causes uncertainties in the measurement. We note here that the error $\delta\mathbf{q}$ could be reduced by using the particle position measurement to get an estimate of the incident wave vector $\mathbf{k}_{\text{inc}}$ as the line between the emitter and the particle, and an estimate of the scattered wave vector as the line between the particle and the receiver array. We have not implemented this correction in the results presented here which assumes in the computation of the velocity that $\mathbf{q} = \mathbf{q}_0$ is fixed, both in direction and magnitude. With the geometry of the experiment shown in Fig. 5, one has for the magnitude $q_0 = |\mathbf{q}_0| = \sqrt{2+\sqrt{2}}(2\pi\nu_0/c)$, where ν_0 is the incoming sound frequency, C_0 the sound speed in the fluid and directions between the axis perpendicular the receiver and emitter arrays form an angle equal to $\pi/4$. The direction $\hat{\mathbf{q}}_0 = \mathbf{q}_0/q_0$ is given by the vector addition $\mathbf{k}_{\text{scat}} - \mathbf{k}_{\text{inc}}$, where $\mathbf{k}_{\text{scat}}$ is directed along the x or y axis depending whether the measurement comes from array 1 or array 2, cf. Fig. 5. For the estimation of the variation $\mathbf{q} \pm \delta\mathbf{q}$, we introduce the angular apertures of the emitter and receiver α_E and α_R, respectively. For instance, one may estimate α_E and α_R as the angular width of the first diffraction lobe of emitting and receiving transducers; it yields $\alpha_E = \alpha_R \sim 0.3$ radian at 2.5 MHz. We then let $\mathbf{k}_{\text{inc}}$ and $\mathbf{k}_{\text{scat}}$ vary within α_E and α_R (respectively) of their geometrical orientation. A straightforward calculation shows that the scattering wave vector $\mathbf{q}$ has a maximum variation of amplitude of equal to 5.4% of q_0, while its direction is at maximum at 0.16 rad from $\hat{\mathbf{q}}_0$. The change in the magnitude of $\mathbf{q}$ as a direct, proportional impact on the velocity measurement, which leads to an error on the magnitude of the velocity equal to 4.5% in the case considered here. The angular variation of $\mathbf{q}$ introduces a measurement bias, as it tends to mix the velocity components. Indeed if the particle velocity is perfectly aligned with $\mathbf{q}_0$, the bias is very small ($1 - \cos(0.16\text{ rd}) \sim 1\%$); however it is significant for a particle whose velocity is perpendicular to $\mathbf{q}_0$ ($\sin(0.16\text{ rd}) \sim 16\%$). We wish to stress that the above estimate of the angular variations of $\mathbf{k}_{\text{inc}}$ and $\mathbf{k}_{\text{scat}}$ are really upper limits. In practice, the dynamical range of the detection (transducers/frequency multiplexer/AD converter) limits the measurement to particles that move inside the central region of the measurement domain. The effective angular aperture could therefore be alternatively defined as corresponding to an emission/detection amplitude equal to half the maximum (3 dB attenuation) of the transducers diffraction profile. This reduces the previous estimates of α_E and α_R by 44% and thus the amplitude variation of $\mathbf{q}$ to 4.5% and its direction to variations within 0.06 rad of $\hat{\mathbf{q}}_0$. The error and the bias on the velocity measurement are then of the order of 5%, leading to an upper limit uncertainty equal to 10% of the measured velocity value. All the estimations above neglect the error introduced by the signal processing AML algorithm which is nearly two order of magnitude smaller, as shown in Ref. 21 when its performance was compared to synthetic test signals. In fact, under the assumption that all transducer locations are per-

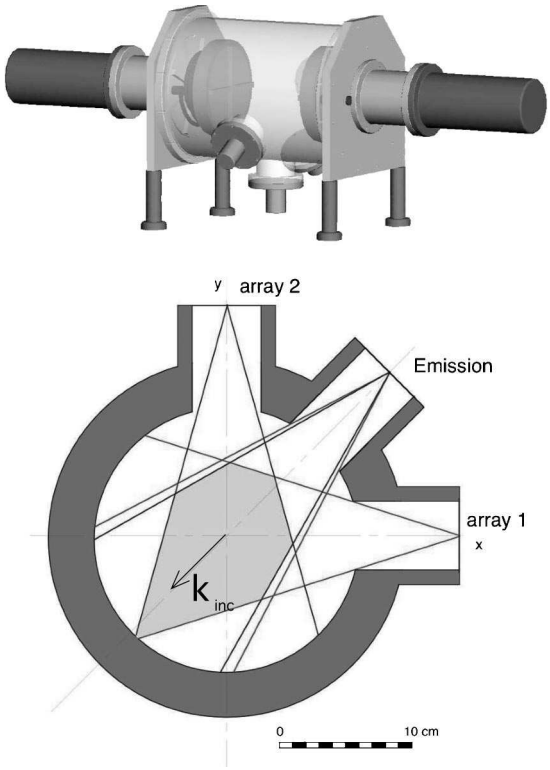

FIG. 5. Experimental setup, von Kármán flow. (Top) Sketch of the experimental apparatus. dc motors drive the counter rotation of the disks. The acoustic transducers lie in the mid-plane, in the geometry shown in the bottom figure. The lines indicate the width of the emission or reception regions for the different transducers (one for emission and two receiving arrays). The measurement volume is the intersection of the 3 cones and is shown as light gray area.

fectly known and that the plane wave model is actually valid, the AML procedure provides as a byproduct an estimate of the error variance on the frequency estimation; it is equal to the inverse of the Hessian measures (cf. figures and detailed calculations in Ref. 15). On signal records for which the SNR is fair, this measure proves to be well below the errors induced by the uncertainty over **q**.

In the estimation of the particle position, the same algorithm has been used. Successive elements in the transducer array are used to build the signal vector subspace, whereas time delayed samples where used for frequency (velocity) tracking—one now estimates a spatial frequency instead of a "temporal" frequency. Errors are then related to the determination of the relative positions of the transducers in the array, and to the performance of the estimation algorithm (the AML assumes plane wave fronts while they are really curved). A first estimation of the AML error is given by the inverse Hessian at the estimated bearing angle. At reasonably high SNR (see records and examples on the figures), this error is below the indeterminacy induced by the errors due to the small number of transducers in each line of the array.

III. APPLICATION TO TURBULENCE MEASUREMENT

A. Experimental setup

In order to be able to follow tracer particles for long times, it is helpful to use a confined flow and to study it in the region where the mean velocity is almost null. The turbulent flow we use is a von Kármán swirling flow: the water is set into motion by two coaxial counter-rotating disks in a cylindrical tank. The flow characteristics are discussed in more detail in Refs. 11 and 15. In our experiments, the cylindrical vessel has a linear dimension of the order of 20 cm, and with disks rotating at frequencies Ω of 5 Hz and above, the Reynolds numbers $\mathrm{Re}=2\pi R^2\Omega/\nu$ exceeds 10^6, where $\nu = 0.8910^{-6}$ m^2 s^{-1} is the kinematic viscosity of water. In the center of the flow, the generated turbulence has statistical characteristics comparable to the ones observed in the largest wind tunnel experiments.[17]

The acoustic transducers are located in the midplane of the cylinder, as shown in Fig. 5. Two receiver cross arrays of 9 transducers are positioned at a 45° angle from an emitter with two piezoelectric elements. Each emits at a different frequency (2.5 MHz and 2.8 MHz), and each receiver array is tuned to one of these frequencies. The wall of the tank and the disks are covered with 3 cm of a sound absorbing material in order to reduced the intensity of echoes. The sound scattered by a moving particle is detected whenever it lies inside a measurement volume—defined as the intersection of the emitting and receiver diffraction lobes—see Fig. 5 (bottom). Using two receiver arrays, we obtain a three-dimensional measurement of the particle position, but only a two-dimensional measurement of the particle velocity. We note that the discs that drive the flow lie outside of the receivers main diffraction lobe; it is important because the moving disks generate echoes with a Doppler shift.

In the sequel, we restrict ourselves to the tracking of the motion of one single tracer particle. The flow is seeded with a very small number of particles (typically between 5 and 7) so that at any one time, only one or two particles move inside the measurement volume. The flow is continuously insonified and the signal for the transducer arrays (after conditioning) is digitized in successive samples of 2^{21} data points. In the data analysis, the portions of the signal where only one particle scatters sound are selected and processed with the AML algorithm to extract the particle motion.

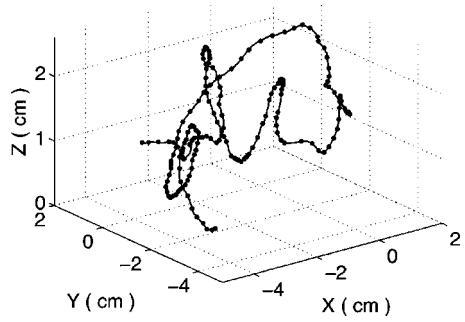

FIG. 6. Example of trajectory recorded in a turbulent flow at a turbulent Reynolds number $R_\lambda \sim 810$ reconstructed from the acoustic measurement.

B. Particle position

The position of the particle is obtained in the following manner: after processing, each receiver arrays give two directions ($D1$) and ($D2$) of sound scattering; the position is defined at the point where the distance between the two lines is at a minimum. An example is shown in Fig. 6. The x and y coordinates lie in the median plane perpendicular to the cylinder axis. They are well determined because the two transducer arrays probe perpendicular direction: the variance of the minimum distance between ($D1$) and ($D2$) in the (x,y) plane is 100 μm, smaller than the particle radius. The z coordinate of the particle (along the cylinder axis) is determined with less accuracy: the variance of the minimum distance between ($D1$) and ($D2$) in the z-direction is about 1.5 mm, much larger than the particle size. In the example shown, the particle is tracked for 0.21 s, which corresponds to 1.5 periods of rotation of the driving disks. One observes violent changes in the direction of motion of the particle. We stress in this example that the particle fluctuating motion is tracked over scales ranging from about 300 μm to 5 cm, i.e. covering over 2 decades. In the context of turbulent flows, this corresponds to an interval between the Taylor microscale and the integral scale of motion.

C. Particle velocity

The velocity of the particle is extracted from the Doppler shift in the scattered sound by the AML algorithm; with two receiver arrays the x and y components of the particle velocity are tracked (axis as shown in Fig. 5). An example of the time variations of one component of the particle velocity has already been given in Fig. 4. The consistency of the measurement with the estimate of the particle position is analyzed in Fig. 7. We show the y component of the particle velocity calculated from the derivative of position (upper curve) and with the AML algorithm (downshifted lower curve). Given the noise that is always introduced in taking the derivative of an experimental signal, we observe that the agreement is

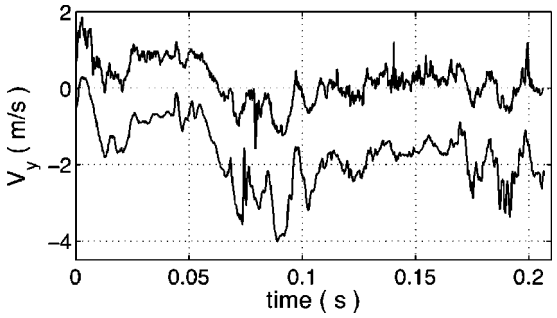

FIG. 7. Example of velocity time series. The top curve is obtained by differentiating the position reconstructed from the relative phase on the transducers. The bottom curve (shifted for clarity) comes from the Doppler frequency shift.

excellent. We also note that the position is estimated with a limited array of transducers, so it is expected that the Doppler detection yield a better estimate of the particle velocity. We can also integrate the velocity signal to obtain the coordinate of the particle. In this case, we find that the variance of the distance between the two estimations is of the order of the particle size.

The dynamics of the measurement is evidenced in Fig. 8 which displays the power spectrum of one component of a 250 μm particle at $R_\lambda = 810$. The left vertical arrow indicates the characteristic frequency of the energy containing scales of the flow (the disks rotation rate). The right vertical arrow indicates the cut-off frequency corresponding to the response of the particle due to its finite size. This value is consistent with the expectation that a particle of size ℓ will not be able to follow motions changing more rapidly than ℓ/u_ℓ, where u_ℓ is the turbulent velocity scale at size ℓ. The horizontal arrow indicates the level under which the noise is dominant. In this case it corresponds to frequencies larger than about 3 kHz, due to the experimental noise and the filtering nature of the AML algorithm. However, we stress that our technique exhibits a dynamical range over 55 dB, with over 2 decades of time resolution. Applied to turbulence, it has yield analysis of Lagrangian motion in the inertial range[18,19] and shows that surprising long-time correlations develop in Lagrangian turbulence.[20] Among other applications, one could use this technique to study the influence of the density of particles on their motion in complex flows.

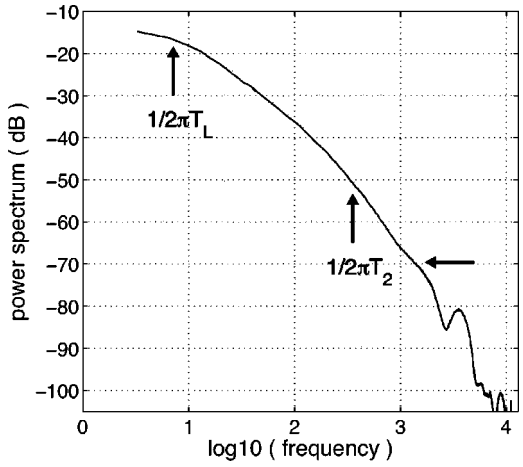

FIG. 8. Power spectrum of the Lagrangian velocity in a turbulent flow at $R_\lambda = 810$. T_L is the Lagrangian integral time scale, T_2 is the time response of the 250 μm particle considered here. The horizontal arrow indicates the level under which the noise becomes dominant.

ACKNOWLEDGMENT

This work was partially supported by ACI Grant No. 2226 from the French Ministère de l'Éducation Nationale et de la Recherche.

[1] H. H. Bruun, *Hot-Wire Anemometry: Principles and Signal Analysis* (Oxford University Press, Oxford, 1995); B. M. Watrasiewicz, *Laser Doppler Measurements* (Butterworths, London, 1976).
[2] M. Raffel, C. E. Willert, and J. Kompenhans, *Particle Image Velocimetry: A Practical Guide (Experimental Fluid Mechanics)* (Springer, Berlin, 1998); *Particle Image Velocimetry—Progress Towards Industrial Applications*, edited by M. Stanislas, J. Kompenhans, and J. Westerweel (Kluwer Academic, Dordrecht, 2000), Vol. 56.
[3] B. Tao, J. Katz, and C. Meneveau, J. Fluid Mech. **457**, 35 (2002).
[4] R. A. Shaw and S. P. Oncley, Atmos. Res. **59–60**, 77 (2001); G. Falkovich, A. Fouxon, and M. G. Stepanov, Nature (London) **419**, 151 (2002).
[5] *UTAM Symposium on Turbulent Mixing and Combustion*, edited by A. Pollard and S. Candel, in Proceedings of the IUTAM Symposium, Kingston, Ontario, Canada, June 3–6, 2001, Fluid Mechanics and its Applications (Kluwer Academic, Dordrecht, 2002), Vol. 70.
[6] A. Pumir, B. Shraiman, and M. Chertkov, Phys. Rev. Lett. **85**, 5324 (2000).
[7] M. Rivera, P. Vorobieff, and R. E. Ecke, Phys. Rev. Lett. **81**, 1417 (1998); M.-C. Jullien, J. Paret, and P. Tabeling, *ibid.* **82**, 2872 (1999); H. Kellay and W. I. Goldburg, Rep. Prog. Phys. **65**, 845 (2002).
[8] S. Ott and J. Mann, J. Fluid Mech. **422**, 207 (2000).
[9] M. Virant and T. Dracos, Meas. Sci. Technol. **8**, 1539 (1997).
[10] G. A. Voth, K. Satyaanarayan, and E. Bodenschatz, Phys. Fluids **10**, 2268 (1998).
[11] N. Mordant, E. Leveque, and J.-F. Pinton, New J. Phys. **6**, 34 (2004).
[12] Y. Takeda, Int. J. Heat Fluid Flow **7**, 313 (1986).
[13] N. Mordant and J.-F. Pinton, Eur. Phys. J. B **18**, 343 (2000).
[14] H. Tennekes and J.-L. Lumley, *A First Course in Turbulence* (MIT Press, New York, 1972).
[15] N. Mordant, O. Michel, and J.-F. Pinton, J. Acoust. Soc. Am. **112**, 108 (2002).
[16] B. Dernoncourt, J.-F. Pinton, and S. Fauve Physica D **117**, 181 (1998).
[17] J.-F. Pinton and R. Labbé, J. Phys. II (France) **4**, 1461 (1994); N. Mordant, J.-F. Pinton, and F. Chillà, *ibid.* **7**, 1 (1997); A. La Porta, Greg A. Voth, F. Moisy, and E. Bodenschatz, Phys. Fluids **12**, 1485 (2000).
[18] N. Mordant, O. Michel, P. Metz, and J.-F. Pinton, Phys. Rev. Lett. **87**, 214501 (2001).
[19] L. Chevillard, S. G. Roux, N. Mordant, E. Levêque, J.-F. Pinton, and A. Arnéodo, Phys. Rev. Lett. **91**, 214502 (2003).
[20] N. Mordant, J. Delour, A. Arnéodo, O. Michel, and J.-F. Pinton, Phys. Rev. Lett. **89**, 254502 (2002).
[21] N. Mordant, Ph.D. thesis, École Normale Suprieure de Lyon, Lyon, November 2001 (unpublished).